energies

MDPI

Article

Thermodynamic Assessment of a Cogeneration System Based on Aluminium–Water Reaction for Hydrogen and Power Production

Lisa Branchini [1], Andrea De Pascale [1], Lorenzini Elena [2,*] and Mariucci Giorgio [2]

[1] Department of Industrial Engineering, University of Bologna, 40100 Bologna, Italy; lisa.branchini2@unibo.it (L.B.); andrea.depascale@unibo.it (A.D.P.)
[2] Interdepartmental Centre for Industrial Research in Renewable Resources, Environment, Sea and Energy, University of Bologna, 40100 Bologna, Italy; giorgio.mariucci2@unibo.it
* Correspondence: elena.lorenzini8@unibo.it

Abstract

This paper presents a conceptual and thermodynamic assessment of an innovative cogeneration system based on the aluminium–water reaction, designed to simultaneously produce hydrogen and electricity. The proposed layout integrates a liquid aluminium combustion chamber with a dual-stage heat recovery section and a steam turbine cycle, enabling the valorisation of industrial aluminium scraps within a circular-economy framework. A steady-state thermodynamic model was developed in Aspen Plus to evaluate system performance under different operating conditions, with a sensitivity analysis on key parameters such as the aluminium-to-water ratio (2.4–4), combustion efficiency, and steam generation cycle parameters. The system performance is investigated in terms of useful output (i.e., hydrogen and electricity production), including a simplified economic evaluation for the assessment of sustainability. Results indicate that, for equivalence ratios ensuring acceptable peak temperatures ($\leq$1700 °C), the system can deliver 2–3 MW of electric power per kg/s of aluminium and achieve cogeneration efficiencies up to 83–87%, assuming a high conversion rate of water into hydrogen (roughly 0.106 kg of produced H_2 per kg of inlet Al, if 95% of mole conversion is considered). The minimum break-even levelized cost of hydrogen is estimated to be 15.7 EUR/kg under current economic conditions.

Keywords: aluminium; hydrogen; waste heat recovery; cogeneration; electrofuels; circular economy; environmental impact; energy conversion

Academic Editor: Zhiqiang Xie

Received: 29 December 2025
Revised: 26 January 2026
Accepted: 28 January 2026
Published: 29 January 2026

1. Introduction

The global energy crisis and the continuous growth in energy demand have intensified the search for renewable and sustainable energy sources. In the EU, primary energy consumption still relies heavily on fossil fuels such as natural gas, oil, and coal, which contribute to air pollution and greenhouse gas emissions [1]. Although renewable sources such as solar and wind power are expanding, they remain costly and subject to intermittency, as highlighted in several reviews [2,3].

Hydrogen has emerged as a promising energy carrier thanks to its high gravimetric energy density—an important advantage for mobile applications, as noted by Verhelst and Wallner [4]—and its low pollutant emissions during combustion. Nevertheless, its widespread adoption is limited by challenges related to storage, transport, safety, and the environmental impact of current production pathways. In particular, the low density of compressed hydrogen makes storage and transportation technically demanding and

energy-intensive [5], while its inherent fire and explosion hazards pose additional safety concerns [6]. Furthermore, well-to-tank emissions can vary significantly depending on the production technology employed, potentially reducing the overall environmental benefits of hydrogen [7]. Currently, fossil fuel-based methods remain dominant for industrial-scale hydrogen production, such as gasification and steam reforming of natural gas, which represents the principal technology accounting for more than 50% of the world's hydrogen production [8]. Whether the fuel is natural gas or coal, the main byproducts of the process consist mainly of CO, H_2, and CO_2, which significantly contribute to the greenhouse effect and global warming. Hydrogen production from carbon-lean and carbon-free energy sources, including renewable electricity, biomass, and metal fuels [9], still faces challenges and methods are under development. In particular, water electrolysis, when fuelled by sustainable energy, can be crucial for achieving carbon neutrality; however, further technical progress and cost reductions are needed to attain scalability and economic feasibility for current technologies. Cogeneration of hydrogen plus other energy harvesting, such as heat, electricity, cold energy, or other fuels from waste materials or residual industrial energy flows in general, can be a promising strategy for energy conversion and storage systems applied in energy-intensive sectors, as in the metal, glass, concrete, and ceramic industries, seeking more sustainable solutions (see some examples of advanced concepts investigated in previous studies by the authors [10–12]).

Since the low environmental impact of hydrogen depends strongly on the source used to produce it, it is undeniable the importance of developing alternative and green paths for obtaining hydrogen. In this perspective, scientific research has moved towards non-organic energy carriers with great interest, looking to use them in the reaction of metals with water as a possible means of achieving zero-carbon hydrogen production. Metals can be reacted with water to release their chemical energy at various power-generation scales and produce hydrogen, which could be utilised in internal combustion engines and fuel cells [5,13]. In these systems the metals are used as electrofuels [9,14,15] and they represent a way to produce energy that overcomes the limits and environmental impacts of common renewable sources, such as high efficiency, ability to be stored for longer periods of time, transportability over long distances, and availability in large quantities. In particular, aluminium exhibits significant potential as an energy carrier due to its high-energy content per unit of mass and volume and its potential to release heat at high-temperature levels, which is compatible with high-performance thermodynamic cycles. Aluminium also has the following features: relatively low-cost, as scrap material; well-established production process; high recyclability; the possibility of pollutant-free combustion; and an intrinsic safety that would allow on-site hydrogen production with a combustion reaction. In more detail, the combustion of aluminium (Al) with water (H_2O) is a very attractive process both for an energy conversion system and for a hydrogen production method due to the low environmental impact and the release of a large amount of energy. When referring to 1 kg of aluminium consumed, the heat released is approximately 17.5 MJ and the amount of hydrogen produced is 0.112 kg. In the process, 1.002 kg of water is needed for the stoichiometric reaction and 1.890 kg of alumina is formed, according to Pini et al. [14]. Thus, the reaction produces hydrogen along with a significant amount of heat and alumina, which can be recycled and retransformed into aluminium in a closed cycle. The residual heat can be valorised through the use of heat recovery systems to also generate electricity.

In this scenario, the current paper focuses on an innovative hydrogen and power production system based on the Al–H_2O reaction, as introduced in previous studies (see Refs. [16,17]), but with a new layout proposed with a particular emphasis on the additional electrical production and the heat recovery optimisation added to the hydrogen generation device. Furthermore, the thermodynamic investigation is accompanied by the first sensitiv-

ity analysis on the economic feasibility of the system. Moreover, compared to the referenced studies, the system considers liquefied aluminium instead of solid particulate. This study starts from and further investigates in depth one of the two configurations presented by Mercati et al. in [18] to convert the heat produced, as consequence of the reaction of Al–H_2O, into useful electrical energy. The process analysed in this study exploits the released combustion heat in the exhaust to generate steam for a power turbine, in the framework of a hydrogen–power cogeneration arrangement. This approach enables the recycling of industrial aluminium scraps, enhancing material and energy recovery, supporting a circular economy, and reducing production and disposal costs.

In particular, the proposed plant layout introduces a further employment of the residual thermal power to pre-heat the reacting water, which was not considered in previous studies compared to the proposed arrangement.

The layout of the proposed system is investigated and evaluated in terms of different operating parameters, by means of simulations modelled through commercial software. The parametric study aims to predict the performance of the innovative aluminium–water system in terms of electrical power output, electrical efficiency, total cogeneration efficiency, and economic feasibility under different operating conditions, with particular focus on the exploitation of heat recovery and minimization of water consumption.

Indeed, the novelty of this work lies in the integration of liquid aluminium combustion with a dual-stage heat recovery configuration, enabling the simultaneous production of hydrogen and electricity within a single thermodynamic framework. Unlike previous studies, which investigated these processes separately or relied on solid aluminium powders, the present system employs liquid aluminium as the reactant and incorporates a dedicated water pre-heating section, thereby enhancing energy recovery and improving overall cogeneration performance. In summary, the main contributions of this study with respect to the existing literature are: (i) the proposal of a novel cogeneration layout based on liquid aluminium combustion coupled with a two-stage heat recovery section; (ii) the development of a thermodynamic model that accounts for realistic non-adiabatic operating conditions; (iii) the combined assessment of hydrogen production, electric power output, and preliminary economic feasibility. These features collectively distinguish the proposed concept from previously investigated aluminium–water systems.

2. Materials and Methods

2.1. Description of the Conceived Process

A conceptual schematic diagram of the considered process is presented in Figure 1, showing the main blocks along with material and energy streams. Both aluminium and water reactants are pre-heated before entering the combustion chamber where the main Al–H_2O reaction occurs, which mainly produces hydrogen and alumina (and residual steam in case of uncompleted reaction). The product stream then proceeds to a heat recovery section where the combustion products are cooled down. This section can be in principle used to produce useful heat or both heat and power. In fact, although the main product of this plant is hydrogen, a predominant role is covered by the profitable usage of the heat released during the combustion process. As described in [18], two different solutions have been proposed to convert the heat produced into useful electrical energy: the first directly using the gaseous combustion products (hydrogen and superheated steam) in a gas turbine; the second exploiting the combustion exhaust thermal power to heat up water in a steam turbine cycle. The proposed system will focus on the second option since it allows one to adopt a combustion chamber working at atmospheric pressure, which is much lower than the pressure values required for a gas turbine configuration. Furthermore, in the steam cycle configuration, the combustion products (in which solid particles are

present) are used in a heat recovery section to superheat a separate steam stream, which subsequently expands in the turbine, not affected by the solid residuals of combustion. A separation section is eventually collocated downstream of the plant, where the hydrogen produced is separated from the solid alumina and the water, which can be recycled back to the combustion chamber in order to minimise the overall water consumption. The separation section is not analysed in detail in this study, while particular focus is put on the thermodynamic aspect of the system.

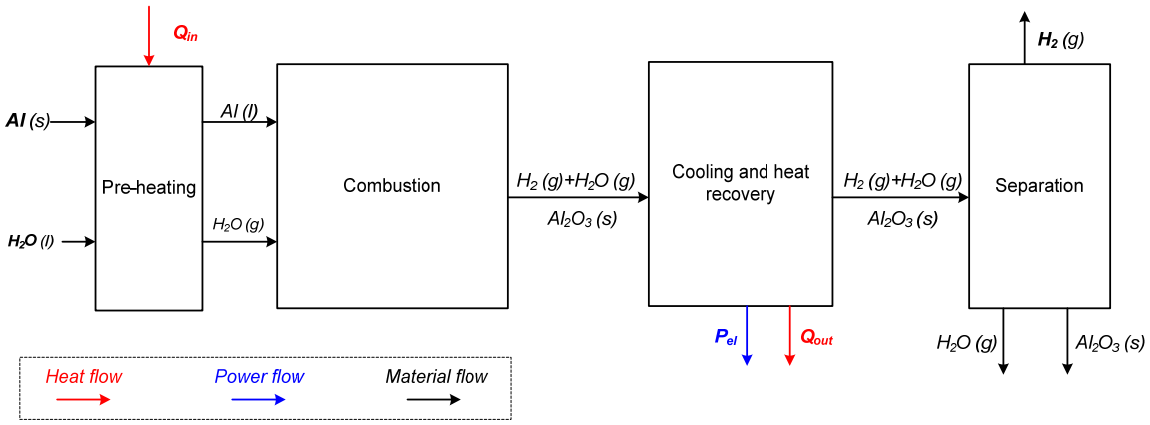

Figure 1. Schematic diagram of the cogenerative process key sections, with the main material and energy flows.

2.2. Energy System Layout

The overall system layout is shown in Figure 2, where the main flow streams are numbered and components are highlighted. It consists of four main sections, namely:

- The aluminium reaction section (section A in Figure 2);
- The gas cooling section for power generation (section B);
- The internal water pre-heating section (section C);
- The gas separation section with the water recycling unit (section D).

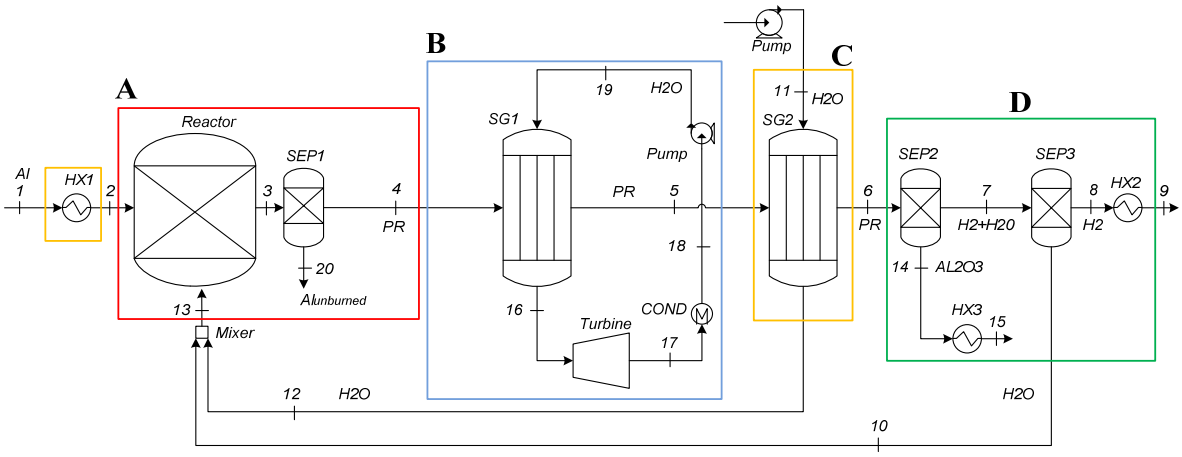

Figure 2. Plant layout of the energy system.

Each section is briefly described below to clarify the flow of material and energy throughout the system. This arrangement allows us to develop a thermodynamic lumped-parameter model of the system, with the main focus on the energy demand and heat exchange of each section.

Aluminium reaction section (A)

In this section, an input stream of aluminium (stream 1 in Figure 2) is fed by an external source of solid material. The solid material at ambient temperature is heated by an external heat source in a heat exchanger (HX1) up to the melting temperature required for entering the combustion section according to the combustor concept analysed by Milani et al. in [19]. The use of liquid aluminium, rather than solid microparticles, avoids the complexities associated with powder production and enables the recycling of industrial aluminium waste, which can reduce the environmental impact of the product life cycle. Moreover, this option prevents the formation of an oxide layer on the aluminium surface and the subsequent activation process [20–22]. The melted aluminium (2) reacts with the slightly superheated water steam (13) in the "Reactor" component, as shown in Figure 2, which represents the combustion chamber. At equilibrium, the stoichiometric reaction equation for solid aluminium and gaseous water reads as follows:

$$2Al(s)+3H_2O(g) \rightarrow Al_2O_3(s)+3H_2(g) - 954.8\frac{kJ}{mol}\ (T = 25\ ^\circ C;\ p = 1\ bar) \quad (1)$$

The total amount of reacting water entering the combustor per unit of input aluminium can be varied, and it is given by the sum of the input external water flow (11–12) and the recirculated water flow rate (10) from the separation section. Downstream of the reactor, the unburned aluminium (20) is then separated from the products (4) in a separation unit (SEP1).

Gas cooling section for power generation (B)

In this section, the high enthalpy content of the combustion products is converted into mechanical power using a steam turbine cycle, which can operate an electric generator. The product stream (PR) exiting the reactor (4) is conveyed to a high-pressure steam generator (SG1) where superheated steam (16) is produced and expands in a steam turbine. Downstream of the turbine, a condenser is used to condensate the exhaust vapour (17) into liquid water (18), and finally a circulating pump is used to obtain the turbine inlet working pressure (19). The water steam mass flow rate produced in SG1 and the generated power are calculated as a function of the combustion conditions (i.e., temperature of combustion products).

Water pre-heating section (C)

In this section, a further exploitation of the residual heat of the products (5) is realised in a second steam generator (SG2). This heat exchanger vaporises an external water stream (11), which is subsequently mixed with the recirculated superheated steam (10) before entering the combustion chamber (13). Thus, the SG2 component produces the make-up steam consumed by the aluminium combustion process, utilising the residual heat content of the combustion products after the SG1 unit.

Separation section (D)

In the final section of the system, two separation steps are considered. At first the alumina (14) is separated from the gaseous phase products (7) in order to remove the residual solid phase. Then the hydrogen (8) is separated from the excess water resulting from combustion (10). The separated water flow rate (10) mixed with the external flow (12) is recirculated to the combustion chamber. The separated alumina (14) and hydrogen (8) streams are subsequently cooled to ambient temperature by additional heat exchangers (HX3 and HX2), and the residual heat can be further utilised. The output hydrogen stream (9) could eventually be conveyed to a storage system or to other direct valorisation processes.

2.3. Operating Conditions

The performance assessment of the entire system was addressed, considering the influence of key size and operating parameters of the main components. Concerning the combustion chamber, the main characteristic parameter is represented by the reacting temperature, which is mainly affected by the inlet aluminium–water ratio. In particular, in order to characterise the combustion process, in this study the following equivalence ratio (λ) definition, reporting the normalised oxidizer/fuel ratio, is considered:

$$\lambda = \frac{\left(\frac{\dot{m}_{H2O}}{\dot{m}_{Al}}\right)}{\left(\frac{\dot{m}_{H2O}}{\dot{m}_{Al}}\right)_{stoic}} \quad (2)$$

where $\dot{m}_{H2O}$ is the combustor inlet mass flow rate, $\dot{m}_{Al}$ the aluminium mass flow rate, and $(\dot{m}_{H2O}/\dot{m}_{Al})_{stoic}$ is the reaction stoichiometric ratio (based on Equation (1)). Despite the lack of a large dataset of experimental data on the aluminium–water combustion process, Figure 3 depicts the influence of the equivalence ratio on the temperature developed during the reaction (T_{CC}), as reported in some of the available literature references [17,23,24] and mainly obtained through flame modelling with reduced chemistry mechanisms. It is interesting to notice that, in the range of λ close to the stoichiometric value, the expected combustion flame temperature values are extremely high (close or above 3000 K) and not compatible with conventional combustor materials. Values of λ above 2.4–2.5 are considered reasonably acceptable (temperature drops below 2400 K) for the combustor and the downstream components. If indeed λ is too high, the water excess can cause a significant temperature drop, while values of $\lambda < 1$ result in a lack of water and unacceptable rates of unburned aluminium. For this reason, the value of λ considered in the current analysis has been limited to the range of 2.4 to 4.

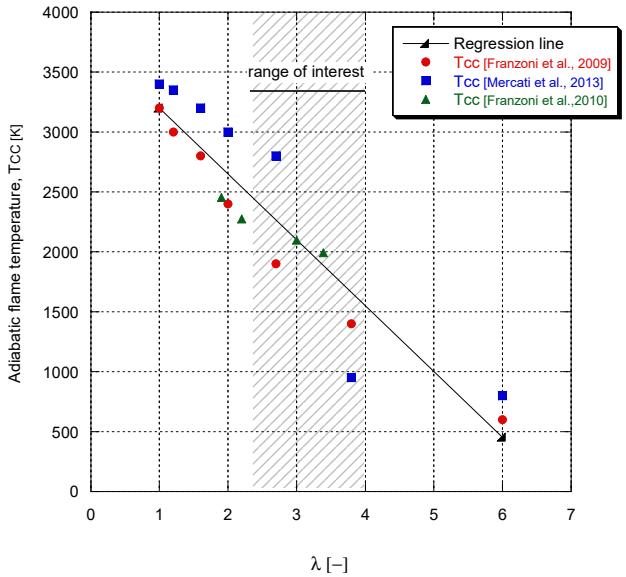

Figure 3. Adiabatic flame temperature value as a function of the normalised oxidizer/fuel ratio according to different sources: *Tcc* from Franzoni et al. (2009) [24], from Mercati et al. (2013) [23], and from Franzoni et al. (2010) [17].

It is important to clarify that the temperatures displayed in Figure 3 result from a comparison between those presented in different studies. The temperature values reported in [17] were calculated for different Al–H_2O mass flow ratios, using the EQUIL code of the Chemkin-2 library [25], while temperature values in [23] were obtained through a numerical model created with the LMS Imagine LabAMESim code [26]. Finally, the

analysis carried out in [24] consisted of the construction of a detailed kinetic mechanism for Al–H_2O reactions (based on data from different sources, for example, [27]) which was used in the simulations based on the SENKIN code. Figure 3 also includes a mean trend line representing the linear trend (obtained through least-squares linear regression).

Since the temperatures in the combustion must remain within a range of values that can be realistically tolerated by the combustor, the values in [24] have been taken as references for setting the temperatures in the subsequent simulations. The variation of λ affects the temperatures of the products (T_4), which in turn determine the steam flow rates in the steam generator and consequently the electrical power produced.

Concerning the power generation section (B) in Figure 2, a superheated steam turbine cycle has been considered, imposing the steam thermodynamic properties at the turbine inlet according to the state of the art of conventional steam cycles. The steam production at SG1 is regulated by the exhaust gas conditions in (4) and the outlet temperature (5) set in SG1. These temperature boundary conditions affect the water pre-heating section (C) steam production. Eventually, the separation section (D) operating conditions are designed by assuming a fixed temperature and separation yield for each stage of separation.

The system has been modelled using a lumped-parameter approach to assess its potential energy performance and optimise its design through a parametric investigation. In particular, the conceived integrated system can be considered as a cogeneration energy system, producing both hydrogen and power (plus possibly residual heat) from the initial aluminium feedstock.

3. Numerical Analysis

3.1. Software Implementation

An energy model of the thermodynamic system was implemented in ASPEN Plus^{TM} [28], a commercial tool for numerical lumped-parameter modelling of complex energy systems. The model is aimed to predict, in a steady-state condition, the performance of the system, taking into account the main chemical reactions and mass and energy balances. The implementation of the system layout in the software graphical interface is portrayed in Figure 4, using standard components such as chemical reactor, heat exchangers, pumps and turbine units, and other auxiliary components (separators, mixers, etc.). In particular, the combustion chamber is modelled with a conversion reactor, a separator which simulates the removal of the unconverted fuel, and a downstream heat exchanger (HX4 in Figure 4) in order to take into account the heat loss due to combustor cooling and non-adiabatic effects. The liquid aluminium preparation for combustion from the solid material is emulated with a heat adder (HX1 in Figure 4). Both steam generators SG1 and SG2 are simulated with water–gas heat exchangers, thermally designed by setting the hot fluid outlet state (SG1 in Figure 4) and cold fluid outlet state (SG2). The turbines and pumps are designed by setting the related isentropic efficiency parameters. For simplicity, all separation units (SEP1, SEP2, SEP3) were assumed to operate with an ideal 100% removal efficiency, in order to estimate the maximum hydrogen production at the outlet. This assumption does not significantly affect the power generation, while hydrogen output can be affected. Actual separation efficiency values depend on different aspects, including the admitted cost for separation, the implemented sections of separation, and the type of available technology, not analysed in this study. A further analysis could focus on a more realistic data for gas–water–solid separation systems, where the reduced separation efficiency (e.g., values ranging between 90% and 95% could represent a target for the filter design) could result in a proportional lowering of the hydrogen production and could imply the need to consider alumina residuals.

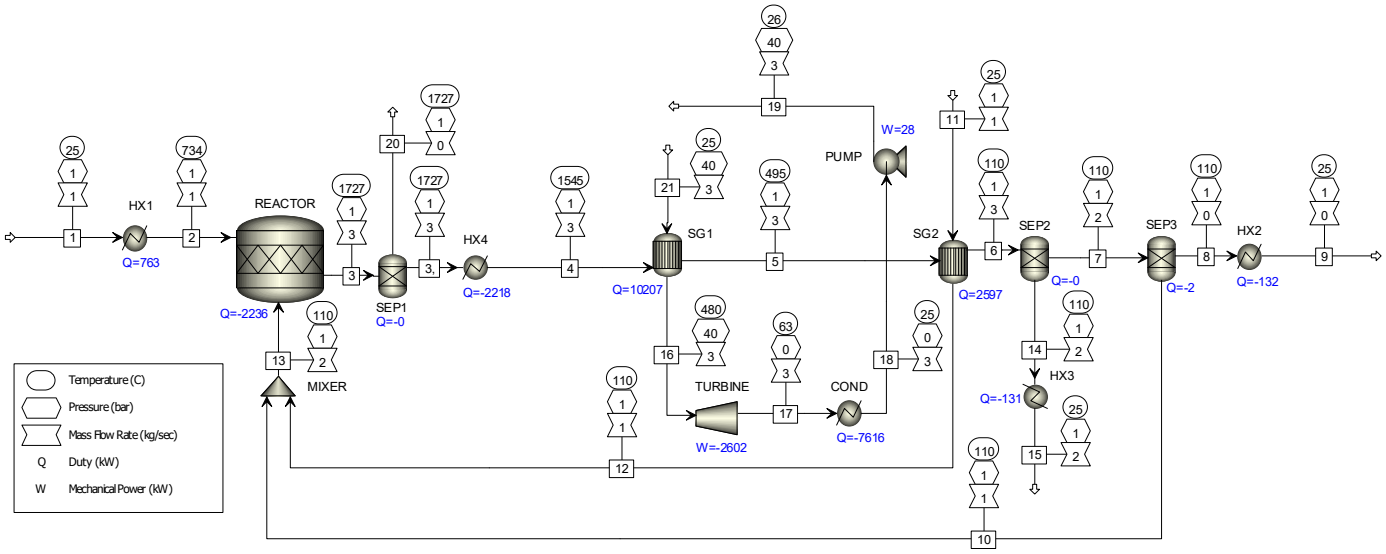

Figure 4. Aspen Plus system model including numerical results (mass flow, temperature, pressure, and power quantity values) obtained corresponding to the design-point operating conditions λ = 2.4.

Figure 4 shows numerical results in terms of temperature, pressure, mass flow rate, exchanged heat, and mechanical power values for each system section, identified by the numbers within the boxes. The values correspond to the operating conditions evaluated at an equivalence ratio of λ = 2.4.

3.2. Input Parameters

The key numerical assumptions used in the simulations are summarised in Table 1. A unit mass flow rate of aluminium at the combustion chamber inlet (1 kg/s) is considered in all the simulations in order to obtain the system performance per unit of inlet feedstock. The liquid aluminium combustor inlet temperature is set to 700 °C, while the inlet water is considered in a slightly superheated state with temperature equal to 110 °C and pressure equal to 1 bar. Parametric simulations were performed by varying the water feed conditions, i.e., the fresh water consumption, calculated as a function of the equivalence ratio (λ) and varied within the range of 2.4 to 4. At the combustor chemical reactor, the one-step direct reaction (1) has been imposed (thus involving only the main combustor products and neglecting intermediate species). Adiabatic temperature is considered from [24] and, in order to account for the non-idealities in the combustion process, two efficiency terms are included, namely a chemical reaction conversion (η_C) and a thermal efficiency (η_d), accounting for the heat dissipation through the combustor walls. This thermal efficiency estimates the heat losses related to the non-adiabatic nature of the combustion device by reducing the product temperature at the combustor outlet (T_4). The overall efficiency of aluminium combustion remains a design-dependent variable in the process, depending on the actual design features of the innovative combustor. In this study, the thermal efficiency term has been varied to account for different geometrical features of the chamber. Three different values of combustor thermal efficiency (η_d) were evaluated, namely 100%, 95%, and 90%, for the purpose of comparison, while a constant η_C value equal to 95% has been fixed for the sake of simplicity, in line with conventional liquid fuel combustors. Furthermore, this study considers a mean value, accounting for the differences occurring in actual combustion across the λ range. The values of product temperature (T_4) subject to thermal efficiency (η_d) are shown in Table 2.

Table 1. Operating parameters of the system.

Sections	Parameters	Values
combustion (A)	Oxidizer/fuel ratio (λ) range	2.4–4
	Aluminium inlet pressure	1 bar
	Aluminium inlet temperature, T_1	25 °C
	Aluminium inlet flow rate	1 kg/s
	Liquid aluminium inlet temperature, T_2	700 °C
	Combustion chamber pressure	1 bar
	Thermal efficiency, η_d	100–90%
	Chemical conversion efficiency, η_C	95%
	Water inlet temperature, T_{13}	110 °C
heat recovery and power generation (B)	Steam turbine inlet temperature, T_{16}	480 °C
	Steam turbine inlet pressure	40 bar
	Steam turbine isentropic efficiency, η_{is}	80%
	Condensation pressure	0.2 bar
water pre-heating (C)	Water inlet temperature, T_{11}	25 °C
	Water inlet pressure, p_{11}	1 bar
	Water inlet flow rate, $\dot{m}_{11} = \dot{m}_{12}$	0.96 kg/s
	Water outlet temperature, T_{12}	110 °C
separation (D)	Temperature of products after separation unit, T_7	110 °C
	Hydrogen cooling temperature, T_9	25 °C
	Alumina cooling temperature, T_{15}	25 °C

Table 2. Adiabatic flame temperature and SG1 to SG2 inlet temperature.

λ [-]	T_{CC} [°C] (η_c = 95%)	T_4 [°C] (η_d = 100%)	T_4 [°C] (η_d = 95%)	T_4 [°C] (η_d = 90%)	T_5 [°C]
2.4	1727	1545	1467	1390	495
2.6	1627	1473	1399	1326	479
2.8	1527	1401	1331	1261	463
3.0	1407	1311	1245	1180	441
3.2	1327	1258	1195	1132	432
3.4	1247	1198	1138	1078	417
3.6	1167	1135	1078	1021	401
3.8	1107	1092	1038	983	392
4.0	1027	1035	984	932	380

The combustor outlet temperature affects the produced steam in SG1. Moreover, the temperature of the product stream at the SG1 outlet (stream 5 in Figure 2) has been set in order to maintain the gas (6) at 110 °C at the separation entry (section D). The circulating water flow rate in SG1 (19) has been varied to accomplish a turbine operating temperature of 480 °C. The steam produced in SG1 expands at 40 bar (as suggested in [17,23]) in the turbine, which is assumed to be working with an isentropic efficiency of 80%. These values are in line with those commonly adopted for steam power units of waste-to-energy facilities [29], where risks of fouling, inherent material compatibility, and cost issues could emerge at higher steam temperature and pressure. Downstream of the expansion, the condensation pressure has been set equal to 0.2 bar, as specified in [16]. The reacting water in the combustion chamber is calculated according to the λ value. It is important to note that the reacting water (13) is the sum of an external renewal amount of water (stream 11) and the recirculated excess water flow rate (stream 10) from SEP3, both flowing at 110 °C. The renewal water (11) per unit of input aluminium flow is constant, and the recirculation water flow rate (10) is varied as a function of λ. The external water flow rate $\dot{m}_{11}$ results

from the combustion efficiency setting. The operating parameters, temperatures, and mass flow rate setup are summarised in Tables 1–3.

Table 3. Normalised water mass flow rates per unit of inlet Al flow.

λ [-]	$\dot{m}_{11}$ [kg/s]	$\dot{m}_{10}$ [kg/s]	$\dot{m}_{13}$ [kg/s]	$\dot{m}_{19}$ [kg/s]
2.4	0.96	1.47	2.43	3.01
2.6	0.96	1.63	2.59	2.91
2.8	0.96	1.81	2.77	2.82
3.0	0.96	2.08	3.04	2.72
3.2	0.96	2.20	3.16	2.61
3.4	0.96	2.41	3.37	2.54
3.6	0.96	2.67	3.63	2.48
3.8	0.96	2.82	3.78	2.41
4.0	0.96	3.04	4.0	2.32

4. Results

4.1. Thermodynamic Performance Parameters

To evaluate the system performance under variable operating conditions, the following energy-related quantities were calculated:

- The hydrogen chemical power (F_{H2}), namely the primary output of the system, defined as follows:

$$F_{H2} = LHV_{H2} \cdot \dot{m}_{H2} \tag{3}$$

where $\dot{m}_{H2}$ is the produced hydrogen mass flow rate value (stream 9 in Figure 2), which depends on the aluminium flow ($\dot{m}_{Al}$) and conversion efficiency (η_C).

- The input aluminium energy contribution (F_{Al}), which is as follows:

$$F_{Al} = LHV_{Al} \cdot \dot{m}_{Al} \tag{4}$$

where the aluminium lower heating value (LHV_{Al}) and aluminium mass flow ($\dot{m}_{Al}$) are included.

- The system net electrical power output (P_{el}), defined as follows:

$$P_{el} = \dot{m}_{H2O,turb} \cdot \Delta h_{is} \cdot \eta_{is} \cdot \eta_O \tag{5}$$

where $\dot{m}_{H2O,\,turb}$ is the steam turbine flow rate, Δh_{is} is the turbine isentropic specific work, η_{is} is the turbine isentropic efficiency, and η_O is the steam cycle organic efficiency equal to 95%, in line with medium-size steam power plants [29]. This term accounts, with a holistic approach, for the power used for auxiliaries, for the effect of the main pressure losses, and for minor miscellaneous losses, as solid transportation.

- The associated electrical efficiency (η_{el}), calculated as follows:

$$\eta_{el} = \frac{P_{el}}{F_{Al}} \tag{6}$$

considering the aluminium energy conversion into electric power output.

- A cogeneration efficiency term (η_{tot}) was also introduced to account for both hydrogen and electricity production as follows:

$$\eta_{tot} = \frac{P_{el} + F_{H2}}{F_{Al}} \tag{7}$$

It should be mentioned that this index quantifies the possibility to convert the aluminium potential energy into two different forms, without accounting for differences in energy quality (exergy).

- Finally, a first-law cogeneration efficiency (η_I) was defined by including residual heat recovery and aluminium pre-heating requirements, resulting in the following:

$$\eta_I = \frac{P_{el} + F_{H2} + Q_{pr}}{F_{Al} + Q_{Al}} \quad (8)$$

where Q_{pr} represents the available residual heat flow recovered by cooling the hydrogen and alumina outlet streams (down to 25 °C) downstream of the gas separation section (in HX3 and HX2), while Q_{Al} is the heat demand to pre-heat the aluminium before the combustion chamber. Since the residual heat is produced at a temperature of 110 °C, Q_{pr} could be provided to a low-/medium-grade heat user to produce an additional cogenerative useful effect.

- Eventually, the heat power recovered at SG1 (Q_{SG1}) and SG2 (Q_{SG2}) is also analysed.

4.2. Thermodynamic Performance Results

The main results are plotted in Figures 5–8. In particular, Figure 5A shows the net electrical power output and thermal power at steam generators SG1 and SG2 per unit of inlet aluminium mass flow versus the oxidizer/fuel ratio for a constant η_d value of 100% (no dispersion through the combustor wall, i.e., ideal case). The maximum specific power production per unit of inlet aluminium flow is achieved at the lowest equivalence ratio and it is equal to 2470 kW/kg$_{Al}$. The decreasing trend versus λ of the recovered power Q_{SG1} is due to the reduction in the steam mass flow rate generated in SG1, due to the decreasing temperature T_4 (while the value of the steam turbine inlet temperature is constant, equal to 480 °C).

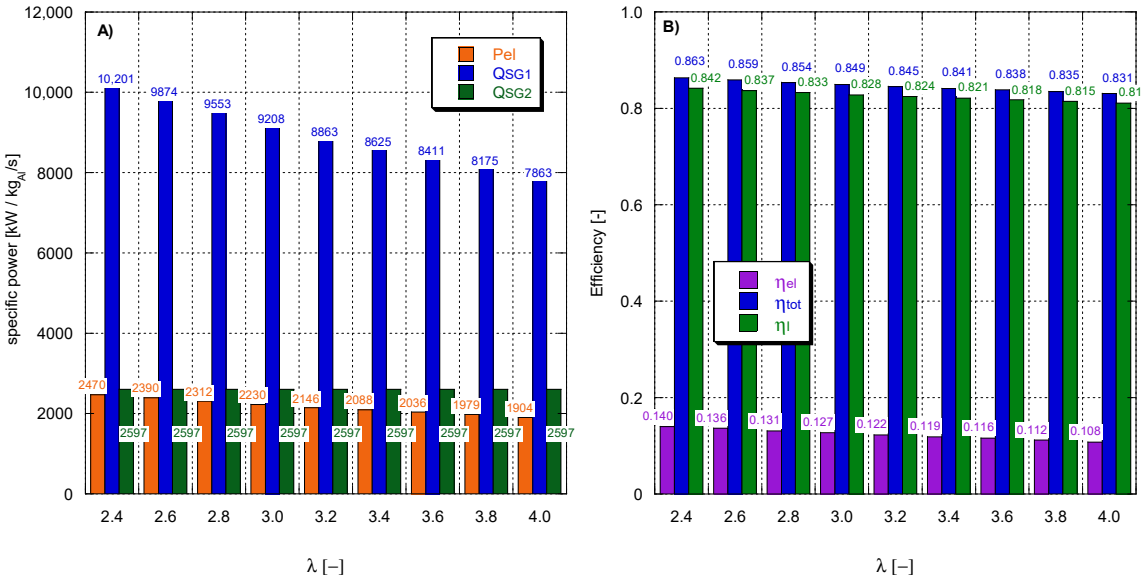

Figure 5. Effect of the oxidizer/fuel ratio on the output electric power and on the heat flow at SG1 and SG2 per unit of inlet aluminium mass flow (**A**) and on the electric and cogeneration efficiency terms (**B**) in the case of η_c = 95% and η_d = 100%.

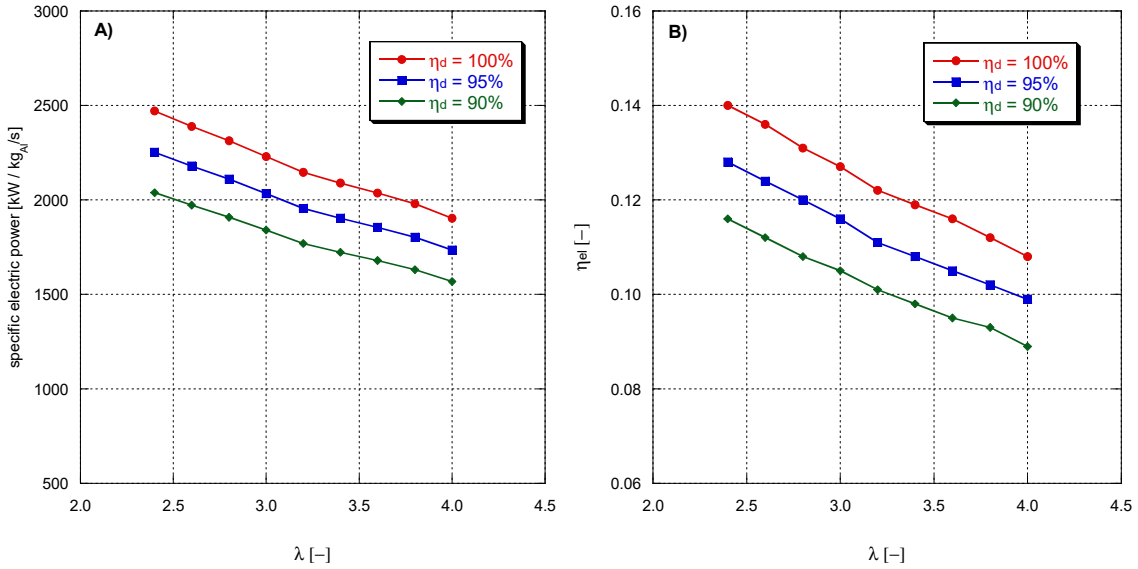

Figure 6. Specific electric power (**A**) and electric efficiency of the steam cycle (**B**) effects of λ and η_d values.

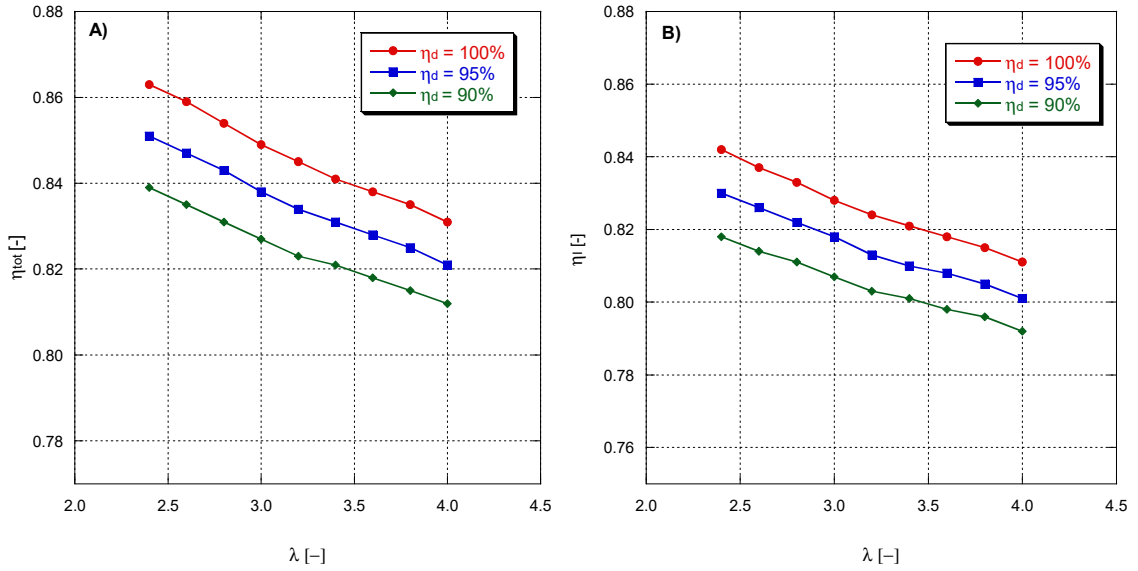

Figure 7. Cogeneration efficiency (**A**) and first-law efficiency (**B**) effects of λ and η_d values.

Figure 5B shows the effect of λ on the obtained system efficiency values. In particular, while the electric efficiency values of the steam cycle are not remarkable (ranging between 11% and 14%), the η_{tot} values are significantly high (above 83%) due to the cogeneration of hydrogen and electricity, and for the high contribution of the hydrogen production rate occurring at high conversion efficiency. The first-law efficiency values are slightly lower than the η_{tot} values, due to the limited impact on performance of the aluminium pre-heating and Q_{pr}. It should be mentioned that the relatively low electric performance derives from the conservative design assumptions adopted for the steam cycle. These values are in line with cases of existing small–medium power plants, such as for the biomass and waste-to-energy plant cases, if conventional materials are used [29].

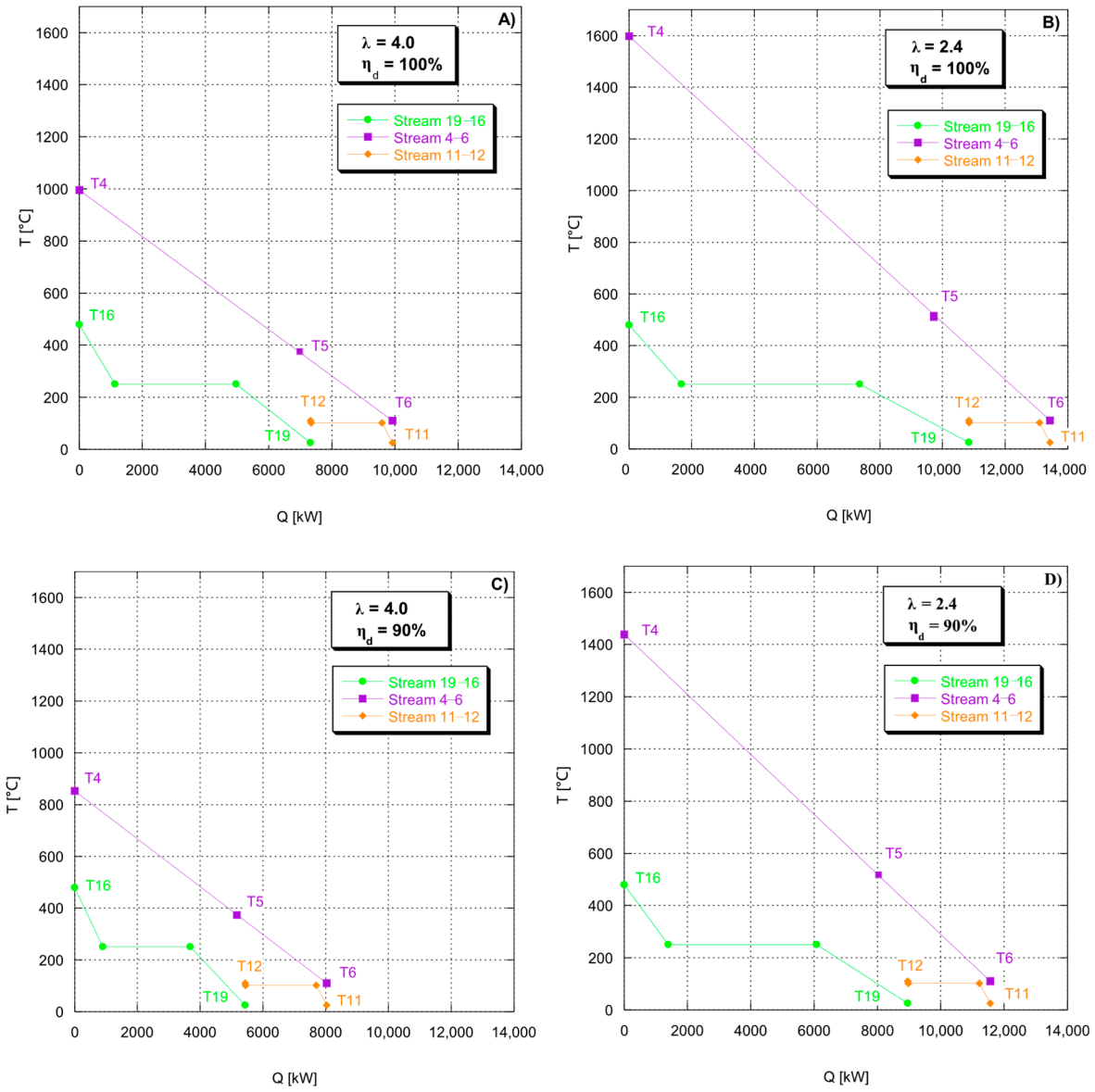

Figure 8. T-Q diagram at SG1 and SG2 for the case: λ = 4 and η_d = 100% (**A**); λ = 2.4 and η_d = 100% (**B**); λ = 4 and η_d = 90% (**C**); λ = 2.4 and η_d = 90% (**D**).

To evaluate the influence of heat losses in the combustion chamber on the system performance, a comparison of three different values of combustor thermal efficiency (η_d), namely 100%, 95%, and 90%, has been carried out. As expected, the system's electric production and the efficiency terms decline with decreasing combustion efficiency (see Figures 6 and 7), since the product's temperature decreases, affecting the generated steam mass flow rate.

The heat exchange diagrams for SG1 and SG2 are presented in Figure 8 for two opposite values of λ and two cases of combustion efficiency. The plot shows that for the adiabatic case (η_d = 100%) the temperature and the heat exchanged are higher compared to the η_d = 90% case, both for the maximum and the minimum λ values (Figure 8). It is noteworthy that the majority of heat exchange occurs in SG1, due to the higher temperature of the combustion products.

In order to optimise the steam cycle in the case with λ = 2.4, showing a large difference between the hot and cold sides at SG1, a further parametric study was performed by varying both the steam temperature (in the range 480–600 °C) and the steam pressure (from 40 bar to 180 bar).

Figure 9 shows the obtained steam cycle performance in terms of specific power per unit of aluminium flow. The steam cycle with a subcritical pressure value of 180 bar and a temperature of 600 °C is the best performing, with an electric power increase of 23.04%. The variation of these parameters significantly improves performance but may present some further implications regarding increases in capital costs, material constraints, and operational safety that will not be discussed in this paper. The maximum value of 600 °C used here is in line, but not at the peak, with the current state-of-the-art steam power plants, adopting advanced materials (nickel/chrome-based metal blends) for the superheater section.

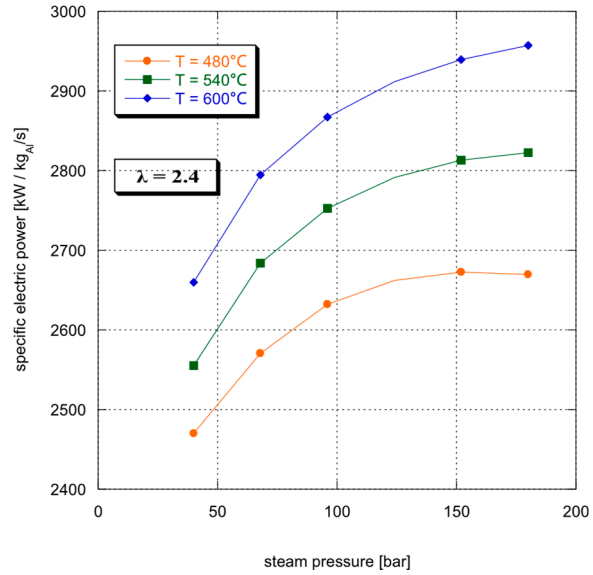

Figure 9. Parametric analysis on steam turbine inlet temperature and pressure values (case of λ = 2.4).

Furthermore, as shown by the T-Q exchange diagram in Figure 10, the ΔT between the cold and hot streams was significantly reduced. It can also be noticed that, for the same thermal power released by the hot stream, the contribution linked to economization increases while the vaporisation decreases since the steam flow rate is reduced.

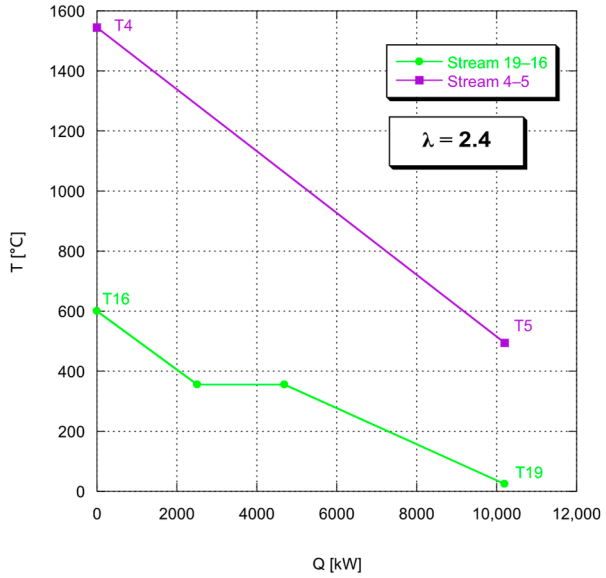

Figure 10. T-Q diagram of the steam generator SG1 for λ = 2.4 at T = 600 °C and p = 180 bar.

Finally, the aluminium conversion efficiency (η_C) was reduced for the two extreme cases of equivalence ratio (λ = 2.4 and λ = 4.0), to assess the effect of the aluminium reactor technology on the system performance. The value of η_C = 75% reported in the experimental study by Barelli et al. [30] was adopted to evaluate the impact of this parameter on the combustion chamber outlet products. The results indicate a proportional reduction in the outlet hydrogen mass fraction and an increase in the water fraction of the same magnitude in both scenarios.

4.3. Preliminary Economic Analysis

The economic performance of the system is primarily influenced by investment and the values of both electricity and hydrogen generation. A preliminary economic evaluation is performed to estimate the value of the electric energy produced by the proposed energy system, primarily due to its fuel consumption, treating the system as an aluminium-fuelled power plant. According to this simplified hypothesis, the cost of electricity (E_C) could be evaluated as:

$$E_C = ME_{Al} \cdot SFC \tag{9}$$

where ME_{Al} represents the market-specific metal price of primary aluminium [EUR/kg] and *SFC* [kg/kWh] is the specific fuel consumption of the system, which relates the aluminium mass flow rate necessary per unit of generated electrical power and is calculated as follows:

$$SFC = \frac{\dot{m}_{Al}}{P_{el}} \tag{10}$$

The energy cost has been evaluated considering the primary aluminium price (ME_{Al}) equal to 2.61 EUR/kg [31]. Figure 11 illustrates a straightforward relationship between λ and the energy cost, which depends on decreasing electric power and subsequently increasing *SFC* values.

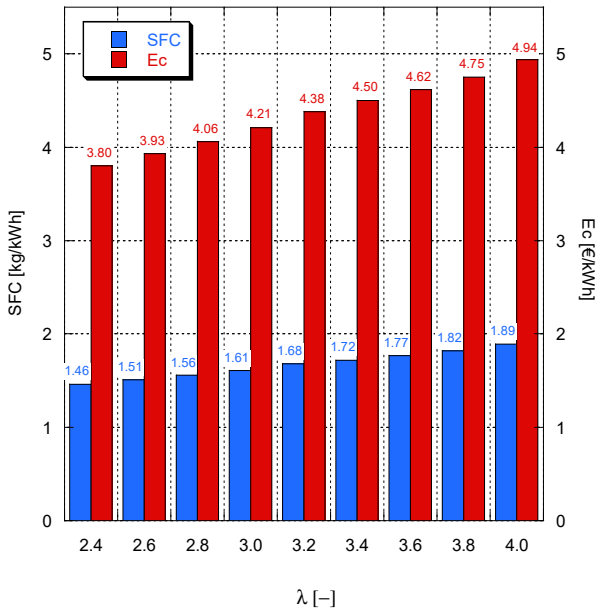

Figure 11. Specific fuel consumption and cost of electricity versus equivalence ratio.

The values of the cost of electricity (in the range of 3.6–4.7 EUR/kWh) obtained with this very simplified approach, which includes only the impact of the "fuel" cost as the main driver of OPEX (i.e., even neglecting all other sources of cost, in the frame of a first rough calculation), are extremely high and not competitive with the current electricity markets, where prices can be one order of magnitude lower. Nevertheless, this approach does not

include the CAPEX and the economic value due to the cogeneration of hydrogen in the economic sustainability of the project.

Thus, a parametric economic analysis was developed to evaluate the profitability of the system for the case $\lambda = 2.4$, considering the initial investment (I_0), the operating costs (OC), and the revenues (R) from both the hydrogen and electricity sales over a multi-year time horizon (n). The net present value (NPV) was then calculated as follows, assuming an appropriate financial discount rate (r) and maintaining all values constant each year:

$$NPV = -I_0 + \sum_{t=1}^{n} \frac{R - OC}{(1+r)^t} \quad (11)$$

The analysis enabled the identification of the break-even hydrogen price assumed here as LCOH (levelized cost of hydrogen), which is defined as the specific selling price (levelized over the time horizon) at which the NPV becomes zero. This value represents the economic threshold above which the project becomes profitable, and it can be considered as a central benchmark for assessing the economic viability of hydrogen production with the proposed plant under the assumed market conditions. The values of the main parameters assumed as reference in the analysis, which are mainly based on the Italian/European market scenario and also following a previous techno-economic analysis by the authors on hydrogen-related systems [32], are summarised in Table 4. In particular, the produced electricity has been initially valorised with a constant electric energy price (EEP) value, basically in line with the Italian national market price (PUN). A sensitivity analysis was also conducted to assess the influence of the EEP value on the economic performance of the system, comparing a current mean EEP value of 132 EUR/MWh in Italy [33] with reduced EEPs (115 EUR/MWh and 0 EUR/MWh) and a raised EEP (150 EUR/MWh).

Table 4. Economic sustainability analysis parameters.

Parameters	Values	Unit
Aluminium (scraps)-specific cost [34]	1.76	EUR/kg
Electric energy reference selling price (PUN) [33]	132	EUR/MWh
Industrial water specific cost	0.002	EUR/kg
Discount rate (r)	3%	-
Plant capacity factor	80%	-
Time horizon (n)	20	years

Concerning the plant investment cost I_0 and the LCOH, these two key and unknown factors have been considered as variables in the break-even-point analysis. The link between the initial investment I_0 (normalised per unit of aluminium mass flow consumption) and the hydrogen specific selling price in break-even conditions is shown in Figure 12.

Based on the performed NPV analysis, the minimum break-even levelized cost of produced H_2 (i.e., at zero investment cost) results equal to approximately 15.7 EUR/kg_{H2} for the reference EEP case. This estimated break-even hydrogen price aligns with the levelized cost ranges for green hydrogen production presented in the Italian National Hydrogen Strategy [35], which identifies costs on the same order of magnitude (approximately 9–16 EUR/kg) across different production and transport scenarios. The break-even I_0-LCOH line shows a steep slope, i.e., a rise in the specific investment cost equal to 10.000 EUR/kg_{Al}/h entails a rise in the levelized cost of hydrogen of almost +1 EUR/kg_{H2}. The results also show a clear relationship between electricity remuneration and the hydrogen break-even price: decreasing the market electricity price leads to a higher value for the break-even hydrogen price and vice versa. If the EEP is lowered to 0 EUR/kWh, the calculated minimum break-even LCOH is equal to 16.7 EUR/kg_{H2}. The influence of

fluctuations in the aluminium market on LCOH can also be highlighted, as shown in the following example: if the price of aluminium scraps is set equal to the price of primary aluminium (2.61 EUR/kg_{Al} [31]) then the break-even levelized cost of hydrogen increases to 23.7 EUR/kg_{H2}, showing a significant impact of the input metal cost on the actual economic performance of the plant. Eventually, the assumed value of the water price within an industrial scenario can vary between less than 1 EUR/t and 3–4 EUR/t, but the impact on the calculated LCOH of the consumed water variation within this range results as less significant than the other factors.

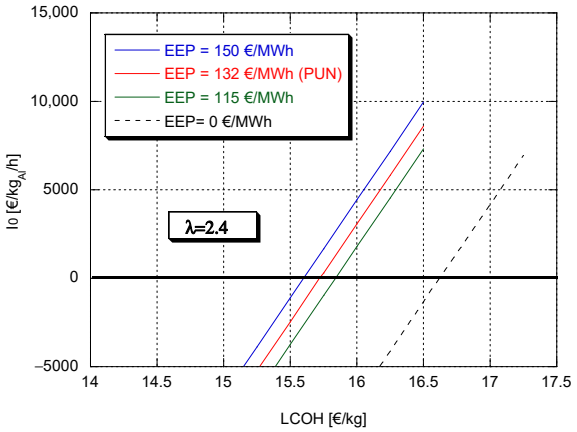

Figure 12. The system break-even specific investment cost vs. the H_2 levelized specific cost, calculated for different electricity energy price values for n = 20 years.

5. Conclusions

This study presents a preliminary assessment of an innovative cogeneration system based on the aluminium–water reaction, designed to simultaneously produce hydrogen and electricity while enabling the valorisation of industrial aluminium scraps. The main research results are as follows:

- The thermodynamic modelling and parametric simulations carried out in this work demonstrate that the proposed concept can operate effectively within a well-defined equivalence ratio range of 2.4–4, ensuring combustion temperatures compatible with conventional materials ($\leq$1700 °C). Within this operating window, the system achieves stable and efficient energy conversion, delivering between 2.0 and 3.0 MW of electric power per kg/s of aluminium, depending on the combustor thermal efficiency, while hydrogen production reaches 0.106 kg of H_2 per kg of aluminium for a conversion efficiency of 95%. As a result, overall cogeneration efficiencies in the range of 83–87% are obtained, exceeding 90% when residual heat recovery is included.
- From a sustainability perspective, the use of liquid aluminium—particularly when sourced from recycled industrial scraps—enhances the circular-economy potential of the proposed system. Nevertheless, several challenges must be addressed before large-scale deployment can be considered. In particular, the scalability of the system is currently limited by the technological maturity of aluminium combustion devices, especially with regard to material resistance at high operating temperatures and the management of reaction by-products.
- The preliminary economic analysis, based on the net present value method, indicates a minimum break-even levelized cost of hydrogen in the range of 15–17 EUR/kg. The results highlight that the economic performance of the system is primarily driven by the capital investment associated with the aluminium conversion unit and, to a lesser extent, by the revenues generated from electricity production. These findings underline the importance of jointly evaluating hydrogen and electricity markets when

assessing the overall economic viability of aluminium-based cogeneration systems. Moreover, the analysis is conducted per unit of input metal flow, in order to be scaled to different plant sizes, but the investigation is performed considering the steam cycle thermal parameters in line with small/medium-size electric power plants, typical of biomass and waste-to-energy power plants. Among the limitations of the presented study, it should also be mentioned that the actual economic performance will be affected by other factors, such as the recovery cost and the market value of the aluminium oxide by-product which are not included but act in opposite directions.

Future research should focus on the experimental validation of the thermodynamic model, with particular emphasis on the verification of (i) combustion temperature, (ii) the actual heat required to prepare liquid aluminium, and (iii) the dissipated heat and their impact on hydrogen yield, in order to confirm the assumptions adopted in the present numerical analysis. Further efforts should also address the optimisation of heat recovery and separation stages, as well as advances in reactor design and high-temperature materials, which will be crucial to fully unlock the potential of metal–water reactions as a viable pathway toward low- and zero-carbon energy systems. In addition, future studies may investigate the direct utilisation of the hydrogen produced by the proposed system in fuel cell technologies (as reported in [36,37]), enabling an integrated power generation configuration and further enhancing overall system efficiency.

Author Contributions: Conceptualization, L.B. and A.D.P.; Funding acquisition, A.D.P.; Methodology, A.D.P., L.E., and M.G.; Data curation, L.E. and M.G.; Investigation, L.E. and M.G.; Formal analysis, L.E. and M.G.; Validation, L.B., A.D.P., L.E., and M.G.; Writing—original draft, L.E. and M.G.; Writing—review and editing, L.B. and A.D.P.; Supervision, L.B. and A.D.P.; Project administration, A.D.P. All authors have read and agreed to the published version of the manuscript.

Funding: This research was funded by PR FESR 2021–2027 Emilia Romagna, grant number CUP: E97G22000590003.

Data Availability Statement: Data supporting reported results can be accessed upon request to authors.

Acknowledgments: This study was conducted within the "MetalH2" Project, PR FESR 2021–2027 Emilia Romagna, which was cofounded by the European Union. CUP: E97G22000590003.

Conflicts of Interest: The authors declare no conflicts of interest.

Nomenclature

Acronyms and subscripts

Al	Aluminium
COND	Condenser
H_2	Hydrogen
H_2O	Water
HX	Heat exchanger
PR	Product stream
PUN	National electric energy selling price
SEP	Separation unit
SG	Steam generator
stoic	Stoichiometric
turb	Turbine

Symbols

Δh_{is}	Isentropic specific work [kJ/kg]	Q	Thermal power [kW]
ΔT	Temperature differential [°C]	r	Financial discount rate [-]
E_C	Energy cost [EUR/kWh]	R	Revenue [EUR]
EEP	Electric energy price [EUR/kWh]	SFC	Specific fuel consumption [kg/kWh]
F	Chemical power [kW]	T	Temperature [°C]
I_0	Initial investment [EUR]	T_{CC}	Adiabatic flame temperature [°C]
LCOH	Levelized cost of hydrogen [EUR/kg]	λ	Equivalence ratio [-]
LHV	Low heating value [kJ/kg]	η_C	Chemical conversion efficiency [%]
$\dot{m}$	Mass flow [kg/s]	η_d	Thermal efficiency [%]
ME	Primary market price [EUR/kg]	η_{el}	Electric efficiency [%]
n	Time horizon [years]	η_I	First-law conversion efficiency [%]
NPV	Net present value [-]	η_{is}	Isentropic efficiency [%]
OC	Operating costs [EUR]	η_O	Organic efficiency [%]
p	Pressure [bar]	η_{tot}	Cogeneration efficiency [%]
P_{el}	Electric power [kW]		

References

1. Eurostat, Energy Statistics—An Overview—Statistics Explained—Eurostat. Available online: https://ec.europa.eu/eurostat/statistics-explained (accessed on 1 May 2025).
2. Jacobson, M.Z. Review of solutions to global warming, air pollution, and energy security. *Energy Environ. Sci.* **2008**, *2*, 148–173. [CrossRef]
3. Muradova, N.Z.; Veziroglu, T.N. "Green" path from fossil-based to hydrogen economy: An overview of carbon-neutral technologies. *Int. J. Hydrog. Energy* **2008**, *33*, 6804–6839. [CrossRef]
4. Verhelst, S.; Wallner, T. Hydrogen-fueled internal combustion engines. *Prog. Energy Combust. Sci.* **2009**, *35*, 490–527. [CrossRef]
5. Bergthorson, J.M.; Goroshin, S.; Soo, M.J.; Julien, P.; Palecka, J.; Frost, D.L.; Jarvis, D.J. Direct combustion of recyclable metal fuels for zero-carbon heat and power. *Appl. Energy* **2015**, *160*, 368–382. [CrossRef]
6. Mazloomi, K.; Gomes, C. Hydrogen as an energy carrier: Prospects and challenges. *Renew. Sustain. Energy Rev.* **2012**, *16*, 3024–3033. [CrossRef]
7. Evro, S.; Oni, B.A.; Tomomewo, O.S. Carbon neutrality and hydrogen energy systems. *Int. J. Hydrog. Energy* **2024**, *78*, 1449–1467. [CrossRef]
8. Hosseini, S.E.; Wahid, M.A. Hydrogen production from renewable and sustainable energy resources: Promising green energy carrier for clean development. *Renew. Sustain. Energy Rev.* **2016**, *57*, 850–866. [CrossRef]
9. Liu, T.; Panahi, A. Metal Fuels as Alternative Sources of Energy for Zero Carbon Emission. *IOP Conf. Ser. Earth Environ. Sci.* **2021**, *943*, 012016. [CrossRef]
10. Branchini, L.; De Pascale, A.; Ottaviano, S.; Poletto, C. Application of high-temperature heat pumps in the ceramic tiles manufacturing sector for waste heat harnessing. *Appl. Therm. Eng.* **2025**, *274*, 126694. [CrossRef]
11. Ancona, M.A.; Bianchi, M.; Branchini, L.; De Pascale, A.; Melino, F.; Peretto, A.; Torricelli, N. Systematic comparison of orc and s-co2 combined heat and power plants for energy harvesting in industrial gas turbines. *Energies* **2021**, *14*, 3402. [CrossRef]
12. Bianchi, M.; Bortolani, G.; Cavazzoni, M.; De Pascale, A.; Montanari, I.; Nobili, M.; Peretto, A.; Tosi, C.; Vecci, R. Preliminary Design and Numerical Analysis of a Scrap Tires Pyrolysis System. *Energy Procedia* **2014**, *45*, 111–120. [CrossRef]
13. Bergthorson, J.M. Recyclable metal fuels for clean and compact zero-carbon power. *Prog. Energy Combust. Sci.* **2018**, *68*, 169–196. [CrossRef]
14. Pini, M.; Breglia, G.; Venturelli, M.; Montorsi, L.; Milani, M.; Neri, P.; Ferrari, A.M. Life cycle assessment of an innovative cogeneration system based on the aluminium combustion with water. *Renew. Energy* **2020**, *154*, 532–541. [CrossRef]
15. Ababneh, H.; Hameed, B.H. Electrofuels as emerging new green alternative fuel: A review of recent literature. *Energy Convers. Manag.* **2022**, *154*, 115213. [CrossRef]
16. Franzoni, F.; Mercati, S.; Milani, M.; Montorsi, L. Operating maps of a combined hydrogen production and power generation system based on aluminium combustion with water. *Int. J. Hydrog. Energy* **2011**, *36*, 2803–2816. [CrossRef]
17. Franzoni, F.; Milani, M.; Montorsi, L.; Golovitchev, V. Combined hydrogen production and power generation from aluminum combustion with water: Analysis of the concept. *Int. J. Hydrog. Energy* **2010**, *35*, 1548–1559. [CrossRef]
18. Mercati, S.; Milani, M.; Montorsi, L.; Paltrinieri, F. Design of the steam generator in an energy conversion system based on the aluminum combustion with water. *Appl. Energy* **2012**, *97*, 686–694. [CrossRef]

19. Milani, M.; Montorsi, L.; Paltrinieri, F.; Stefani, M. Experimental and numerical analysis of the combustor for a cogeneration system based on the aluminum/water reaction. *Energy Convers. Manag.* **2014**, *87*, 1291–1296. [CrossRef]
20. Kaur, P.; Verma, G. A critical assessment of aluminum-water reaction for on-site hydrogen powered applications. *Mater. Today Energy* **2024**, *40*, 101508. [CrossRef]
21. Xiao, F.; Yang, R.; Liu, Z. Active aluminum composites and their hydrogen generation via hydrolysis reaction: A review. *Int. J. Hydrog. Energy* **2021**, *47*, 365–386. [CrossRef]
22. Irankhah, A.; Mohsen, S.; Fattahi, S.; Salem, M. Hydrogen generation using activated aluminum/water reaction. *Int. J. Hydrog. Energy* **2018**, *43*, 15739–15748. [CrossRef]
23. Mercati, S.; Milani, M.; Montorsi, L.; Paltrinieri, F. Optimization of the working cycle for a hydrogen production and power generation plant based on aluminium combustion with water. *Int. J. Hydrog. Energy* **2013**, *38*, 7209–7217. [CrossRef]
24. Franzoni, F.; Milani, M.; Montorsi, L.; Golovitchev, V. *A Novel Concept for Combined Hydrogen Production and Power Generation*; SAE Technical Paper; SAE International: Warrendale, PA, USA, 2009. [CrossRef]
25. Lutz, A.E.; Kee, R.J.; Miller, J.A. *SENKIN: A Fortran Program for Predicting Homogeneous Gas Phase Chemical Kinetics with Sensitivity Analysis*; Sandia Report SAND87-8248; Sandia National Labs: Livermore, CA, USA; Department of Energy: Washington, DC, USA, 1988.
26. Siemens. *LMS-Imagine.LAB*, version 9.0, User Guide LMS-Imagine.LAB AMESim. 2012.
27. Catoire, L.; Legendre, J.-F.; Giraud, M. Kinetic Model for Aluminum-Sensitized Ram Accelerator Combustion. *J. Propuls. Power* **2003**, *19*, 196–202. [CrossRef]
28. ASPEN Plus^{TM}. Available online: https://www.aspentech.com/ (accessed on 10 November 2025).
29. Bianchi, M.; Branchini, L.; De Pascale, A. Combining waste-to-energy steam cycle with gas turbine units. *Appl. Energy* **2014**, *130*, 764–773. [CrossRef]
30. Barelli, L.; Trombetti, L.; Di Michele, A.; Gammaitoni, L.; Asenbauer, J.; Passerini, S. Aluminum Steam Oxidation in the Framework of Long-Term Energy Storage: Experimental Analysis of the Reaction Parameters Effect on Metal Conversion Rate. *Energy Technol.* **2022**, *10*, 2200441. [CrossRef]
31. Trading Economics. Available online: https://it.tradingeconomics.com/commodity/aluminum (accessed on 10 November 2025).
32. Ancona, M.A.; Antonucci, V.; Branchini, L.; Catena, F.; De Pascale, A.; Di Blasi, A.; Ferraro, M.; Italiano, C.; Melino, F.; Vita, A. Parametric Thermo-Economic Analysis of a Power-to-Gas Energy System with Renewable Input, High Temperature Co-Electrolysis and Methanation. *Energies* **2022**, *15*, 1791. [CrossRef]
33. Gestore Mercati Elettrici. Available online: https://www.mercatoelettrico.org/it-it/Home/Pubblicazioni/Indici-GME/PUNIndexGme (accessed on 27 January 2026).
34. Metaloop. Available online: https://www.metaloop.com/it/scrap-metal-price/italy/aluminium/ (accessed on 1 December 2025).
35. Ministero dell'Ambiente e della Sicurezza Energetica. Available online: https://www.mase.gov.it/portale/documents/d/guest/strategia_idrogeno-pdf (accessed on 11 January 2026).
36. Barelli, L.; Baumann, M.; Bidini, G.; Ottaviano, P.A.; Schneider, R.V.; Passerini, S.; Trombetti, L. Reactive Metals as Energy Storage and Carrier Media: Use of Aluminum for Power Generation in Fuel Cell-Based Power Plants. *Energy Technol.* **2020**, *8*, 2000233. [CrossRef]
37. Qi, W.; Yua, L.; Tanga, X.; Wu, J.; Zhanga, Y.; He, Z. Multi-objective optimization of a hydrogen-fueled PEMFC with multi wavy channels via machine learning and CFD simulation. *Int. J. Hydrog. Energy* **2026**, *199*, 152748. [CrossRef]